

Generating himawari-8 time series data for meteorological application

Ahmad Luthfi Hadiyanto^{1,7}, Ketut Wikantika^{2,3}, Ary Setijadi Prihatmanto^{4,5},
Nurjanna Joko Trilaksono⁶, Dedi Irawadi⁷

¹Doctoral Program of Geodesy and Geomatics Engineering, Faculty of Earth Science and Technology, Bandung Institute of Technology, Bandung, Indonesia

²Department of Geodesy and Geomatics Engineering, Faculty of Earth Science and Technology, Bandung Institute of Technology, Bandung, Indonesia

³Center for Remote Sensing, Bandung Institute of Technology, Bandung, Indonesia

⁴School of Electrical Engineering and Informatics, Bandung Institute of Technology, Bandung, Indonesia

⁵Research Center on Information and Communication Technology, Bandung Institute of Technology, Bandung, Indonesia

⁶Atmospheric Science Research Group, Bandung Institute of Technology, Bandung, Indonesia

⁷Aeronautics and Space Research Organization, National Research and Innovation Agency, Jakarta, Indonesia

Article Info

Article history:

Received Jun 21, 2022

Revised Oct 19, 2022

Accepted Oct 24, 2022

Keywords:

Aggregation
Remote sensing
Spatial interpolation
Thermal bands
Time series

ABSTRACT

Optical remote sensing images have been widely used for temporal monitoring. The data is acquired by sensors on satellites with better spatial resolution compared to in-situ measurements by meteorological stations. The problem with utilizing optical images is the cloud, which blocks the ground and near-ground information collected by satellites. To overcome this problem, especially when dealing with thermal bands, we propose a procedure including aggregation and spatial interpolation methods to obtain time series data over a region. There is still no reference to selecting the data period to calculate the aggregate value and apply spatial interpolation. An assessment is proposed by applying Yamane's formula in the time domain and thresholding the number of pixels in the spatial domain. Himawari-8 data was utilized and collected on an hourly basis over Java Island. This algorithm is applied to a sequence of periodic datasets to obtain a time series of aggregate data for meteorological applications. The result of this study is a recommendation to use three-month periods of data over the eastern part of Java.

This is an open access article under the [CC BY-SA](https://creativecommons.org/licenses/by-sa/4.0/) license.



Corresponding Author:

Ahmad Luthfi Hadiyanto

Doctoral Program of Geodesy and Geomatics Engineering, Faculty of Earth Science and Technology

Bandung Institute of Technology

10 Ganeca Street, Bandung, Indonesia

Email: luthfi.hadiyanto@students.itb.ac.id

1. INTRODUCTION

Time series data of dynamic parameters of the earth's environment are commonly used in meteorological applications, for example in climate change monitoring [1]–[3]. For meteorological applications, in-situ data from measurement stations is preferred in many cases to be used as data sources. There will be no problem getting temporal data from meteorological stations. On the other hand, the data does not have good spatial resolution because of the limited number of stations [4].

The utilization of optical remote sensing satellite images has many advantages. The development of its technology is moving forward with continuous development from a lot of providers. The data itself covers the whole world with high spatial resolution and high temporal resolution. The main problem is cloud

existence [5], which has a high occurrence in Indonesia, although different land areas have different yearly patterns [6]. The clouds will block solar radiation and absorb radiation emitted from the ground. The clouds hide information from the ground and near-ground collected by satellites. To use data from optical satellites, the availability of data should be examined carefully.

When the data is used for land monitoring with little change, mosaic-ing of reflectance bands can be done to remove the clouds [7]. Selected temporal data can also be used directly to monitor land use and land cover change [8], [9]. Aggregation can also be calculated directly, just like the composite vegetation index [10], [11]. When dynamic parameters like weather parameters or any brightness temperature in thermal bands related to weather parameters are observed, the method will be different.

Using remote sensing optical data, reconstruction of brightness temperature is usually proposed. There are several ways to get complete spatial-temporal data. Neteler [12] uses spatial-based reconstruction. The method simulates missing values up to 75%. Aggregation can be performed well right after the interpolation, but the time cost is high for the interpolation process on each image. Spatial-temporal-based reconstruction is more popular. Spatiotemporal kriging is used in [13], but the completeness of each image is not always 100%. He *et al.* [14] uses Bayesian reconstruction with good accuracy, but the time cost is high for a larger-sized image. Temporal-based is another option that shows good results. Zhou *et al.* [15] can be applied to land parameters like land surface temperature with the requirement that there is no abrupt change in the value. This method was approved with a small missing value of up to 21.7%. Therefore, it is difficult to implement the method in Indonesia. Luo *et al.* [16] uses generative adversarial networks to generate samples for training, based on recurrent neural networks applied to meteorological data. Some data was removed to simulate missing information. The method can be applied to satellite data, but the time cost is high because the training operation is done pixel by pixel. The main problem with all these methods is the time cost. In this research, we propose a procedure to generate time series data that can reduce processing time. Instead of trying to reconstruct to get complete data, this research proposes calculating aggregate data for each pixel location in the time domain before performing spatial interpolation. To do that, we propose a procedure of assessment based on the availability of data as the novelty of this research. The assessment is directed at finding the minimum period of data applied to Himawari-8 data to create statistical information via aggregation, which can be spatially interpolated. The period should be repeated to create time series information.

A thermal band containing brightness temperature will be used in the experiment. The interpolation method will be evaluated before being used, and spatial correlation between the result and the related physical parameter will be calculated. Evaluation of the aggregate value of brightness temperature is not in the scope of this research since it is difficult to find other data for comparison.

2. METHOD

In this study, the data was limited to a one-year period, and Java Island was selected as the area of interest. There are two main requirements before applying aggregation and spatial interpolation, namely the amount of available data and its distribution pattern. Homogeneous areas may have a smaller number of samples, but there are still no exact criteria for the distribution pattern in this case. Therefore, the focus of this study is primarily on the availability of data.

Images from the Himawari-8 satellite were used because of their high temporal resolution. The imager is onboard a geostationary satellite and covers the western Pacific region, including the whole Indonesian area. The period of mid-2019 to mid-2020 was selected to simplify the analysis, which was not much affected by complex weather like El Niño and La Niña. The data was processed to level 2 high-resolution cloud analysis information (HCAI), which contains cloud classification information. HCAI data was distributed by the Indonesian Meteorological, Climatological, and Geophysical Agency on an hourly basis. There is some lost data, but the percentage is very low. An algorithm based on the Fundamental Cloud Product and brightness temperature values from Himawari-8 images is used to generate HCAI and distinguish cloud cover as clear, cumulonimbus, dense cloud, upper cloud, middle cloud, cumulus, stratocumulus, or stratus/fog [17].

This research performed two kinds of tests: first in the time domain to find any pixel location with the proper aggregate value, and second in the spatial domain to investigate whether spatial interpolation can be applied. A formula by Taro Yamane (1) to estimate the minimum sample size of a population was used as the first criteria. The requirement to implement the formula with a 95% confidence level was assumed to be fulfilled. The number of no-cloud values at each pixel location in a period should be the same or greater than the number of samples calculated by the formula. No-cloud information can be retrieved from HCAI data, flagged as clear. This step results in an aggregate value on every qualified pixel.

$$n = \frac{N}{1 + Ne^2} \quad (1)$$

N is the size of the population, n is the number of samples, and e is the margin of error. The margin of error is assumed to be 5% to obtain the required confidence level. Yamane's formula has been used in remote sensing applications [18]. The formula was applied in the spatial domain, but in this research the formula will be implemented in the time domain on every pixel location.

The area of interest was divided into eight regions as shown in Figure 1 to represent better spatial distribution. The area was divided by the same degree of longitude. The number of pixels in each area is 1522 (R1), 4100 (R2), 3993 (R3), 2688 (R4), 3943 (R5), 4584 (R6), 3003 (R7), and 2128 (R8). A threshold value of 30% for each region was selected as the second criteria based on previous research on image restoration [19]. The accuracy of the restoration was still acceptable with 70% of the pixels removed. Other research shows that the use of 25% subsamples from sediment depth data results in low accuracy in the prediction of sediment volume [20]. Then the thresholds were calculated as 30% of the number of pixels in each area: 457 (R1), 1230 (R2), 1198 (R3), 807 (R4), 1183 (R5), 1376 (R6), 901 (R7), and 639 (R8). Spatial interpolation can be implemented to aggregate data. Inverse distance weighting (IDW) and Kriging interpolation are examples of widely used spatial interpolation methods. In some cases, the performance of the Kriging technique outperforms that of the IDW [21]–[23], so we will use Kriging interpolation in this research for evaluation.

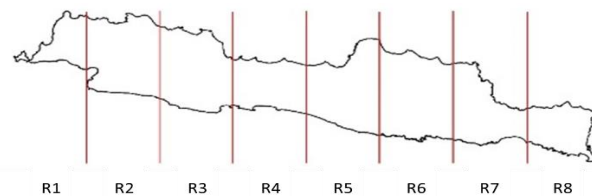


Figure 1. Java Island divided into eight regions

For each region, the test was applied in several scenarios: daily, monthly, three-month period, and six-month period. The algorithm is the same for all scenarios, as shown in Figure 2. The threshold value in the time domain is not fixed based on the length of the period on an hourly basis. A successful region, as shown in the flow chart, means aggregation and spatial interpolated data have the potential to be generated over that region, while a failed region means the contrary.

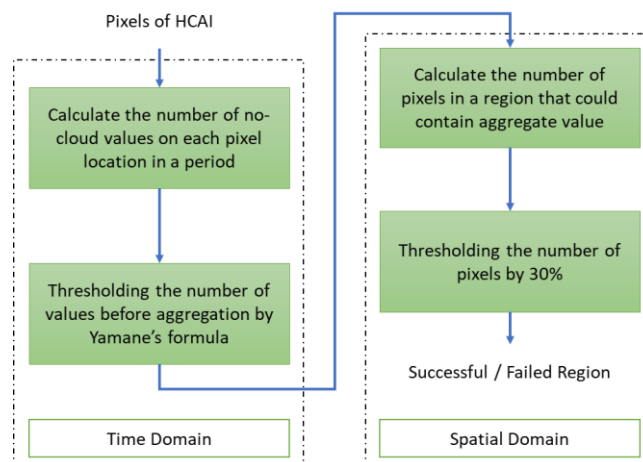


Figure 2. Flow chart of the method

The data ranges from July 2019 to June 2020. A seasonal grouping based on the Asian-Australian monsoon was used and consists of four periods: December-February, March-May, June-August, and September-November. To create a three-month and six-month period of data, it is assumed that data in June 2020 can replace data in June 2019. Yearly variations in cloud coverage in Indonesia are relatively small [6].

Evaluation includes comparison of the results between regions and visual inspection of the spatial distribution of the successful regions. Band 13 of Himawari-8 data is used to represent the dynamic parameter. Band 13 has been used in the algorithm for land surface temperature estimation [24], [25]. Land surface temperature products from Himawari-8 have not been published, therefore we use band 13 for analysis. The result was compared to skin temperature data retrieved from the ERA5 database. Spatial correlation was calculated. Level-1 Himawari-8 data from December to May was used to retrieve spectral data at band 13. Additionally, some of the qualified pixels were used for validation of the spatial interpolation method.

3. RESULTS AND DISCUSSION

3.1. Scenario 1: Daily

With 24 hours per day, the minimum amount of available data in one day as calculated by the (1) is 23. It is defined as the first criteria. The number of pixels which passed the first criteria for each region was then applied to the threshold in the spatial domain as the second criteria. Table 1 shows the number of days every month which passed both criteria in each region. From December up to May, the number of available days is very small. It shows that the occurrence of clouds is very high in the wet season. The number of available days is still not complete in the remaining months.

Table 1. Number of available days passed the criteria

Month	R1	R2	R3	R4	R5	R6	R7	R8
July	0	0	5	2	6	4	5	3
August	1	3	6	0	4	2	1	2
September	2	2	5	1	6	4	3	4
October	0	1	2	0	3	5	4	3
November	1	0	0	0	0	0	1	1
December	0	0	0	0	0	0	0	0
January	0	0	0	0	0	0	0	0
February	0	0	0	0	0	0	0	0
March	0	0	0	0	0	0	0	0
April	0	0	0	0	0	0	0	0
May	0	0	0	0	0	0	1	0
June	0	0	1	0	0	1	2	2

3.2. Scenario 2: Monthly

In a one-month period, the minimum amount of available data to pass the first criteria depends on the number of days in each month. Table 2 shows the number of qualified pixels in each region that passed the first criteria and may contain a monthly aggregate value. All regions passed the second criteria in July-November. In April, only region R8 passed the criteria. In May, there were three regions that passed the criteria, while in June there were seven regions. There is no region that passed the criteria for the full twelve months.

Table 2. Number of qualified pixels by months

Experiment	R1	R2	R3	R4	R5	R6	R7	R8
July	1497	4084	3546	2266	3883	4318	2861	1875
August	1507	4075	3359	2218	3891	4362	2822	1868
September	1519	4098	3502	2296	3888	4420	2867	1945
October	1170	3083	3424	1810	3716	4574	2976	2108
November	1227	1512	2600	1030	2221	4116	2866	2067
December	0	0	0	0	0	0	0	5
January	0	0	0	0	0	0	0	103
February	0	0	0	0	0	0	0	3
March	0	0	0	0	0	0	0	5
April	0	0	0	0	0	0	0	99
May	0	0	0	45	320	1254	759	913
June	38	1429	2438	1777	3594	4279	2893	1909

3.3. Scenario 3: Three-month period

In a three-month period, the minimum amount of available data depends on the number of days in each three-month period. Table 3 shows the number of qualified pixels in each region that passed the first criteria and may contain an aggregate value over a three-month period. Only three regions (R6, R7, and R8) passed the criteria in all periods. Other regions failed to pass the criteria in the December-February period.

Table 3. Number of qualified pixels by three-month periods

Period	R1	R2	R3	R4	R5	R6	R7	R8
June-August	1522	4100	3993	2687	3943	4581	3003	2126
September-November	1522	4100	3990	2671	3943	4584	3003	2128
December-February	0	1	5	14	117	1411	1472	2014
March-May	1362	3557	3703	2506	3897	4562	2988	2123

3.4. Scenario 4: Six-month period

In a six-month period, the minimum amount of available data depends on the number of days in each six-month period. Table 4 shows the number of qualified pixels in each region that passed the first criteria and may contain an aggregate value over a six-month period. All regions passed the criteria, but regions R6, R7, and R8 had already passed the criteria in the previous scenario. The length of six months is chosen rather than four months or five months to obtain seasonal information.

Table 4. Number of qualified pixels by six-month periods

Period	R1	R2	R3	R4	R5	R6	R7	R8
June-November	1522	4100	3993	2688	3943	4584	3003	2128
December-May	1522	4098	3992	2675	3943	4583	2998	2128

3.5. Discussion

The results of the daily and monthly scenarios were very far from fulfilling the criteria, especially in the wet season (December-May). Confidence in creating time series data arises in regions R6, R7, and R8 by applying aggregation and spatial interpolation in three-month periods. The number of qualified pixels in regions R6, R7, and R8 passed the criteria, although the number of qualified pixels in region R6 is very close to the threshold in the December-February period. Figure 3 shows the distribution of the pixels in December-February. Visually, it is shown that the distribution is not fully clustered.

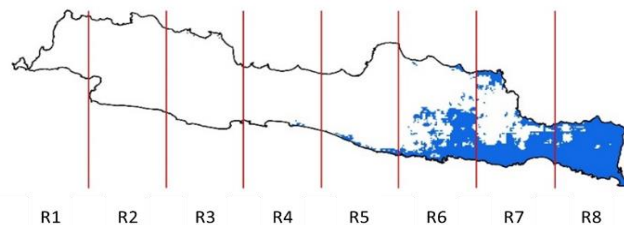


Figure 3. Distribution of qualified pixels in December-February

To evaluate the spatial interpolation method, a dataset of average brightness temperature values is extracted from band 13 of the hourly Himawari-8 images in December-February over successful regions (R6, R7, and R8). The criteria in the time domain were applied to retrieve the average value. The mean value of the average brightness temperature from qualified pixels is 291.5 Kelvin. Spatial interpolation of the ordinary kriging method was applied using 30% of the qualified pixels, selected randomly. The remaining 70% of qualified pixels were used for evaluation. Interpolation resulted in a root mean square error (RMSE) value of 0.3354. The bias was 0.0036, with error values ranging from -2.3256 to 2.6538. Figure 4 shows the spatial distribution of the error value. The RMSE value is low compared to the mean value of the average brightness temperature. The result boosts confidence in obtaining time-series aggregate data of dynamic parameters in regions R6, R7, and R8 over three-month periods using hourly Himawari-8 images.

The spatial correlation coefficient was calculated between the proposed result and skin temperature in regions R6, R7, and R8 to evaluate the entire procedure, including aggregation and spatial interpolation. Brightness temperature data in December-February and March-May was calculated. Monthly skin temperature is used instead of three-months' aggregate to answer the question of whether the longer aggregate data may represent the current condition. The calculation shows that the correlation is high as shown in Table 5 and Figure 5. It means we can use the proposed result in any application related to the skin temperature on the eastern part of Java. Further processing might be applied to have the dynamic parameter extracted from the interpolated brightness temperature values.

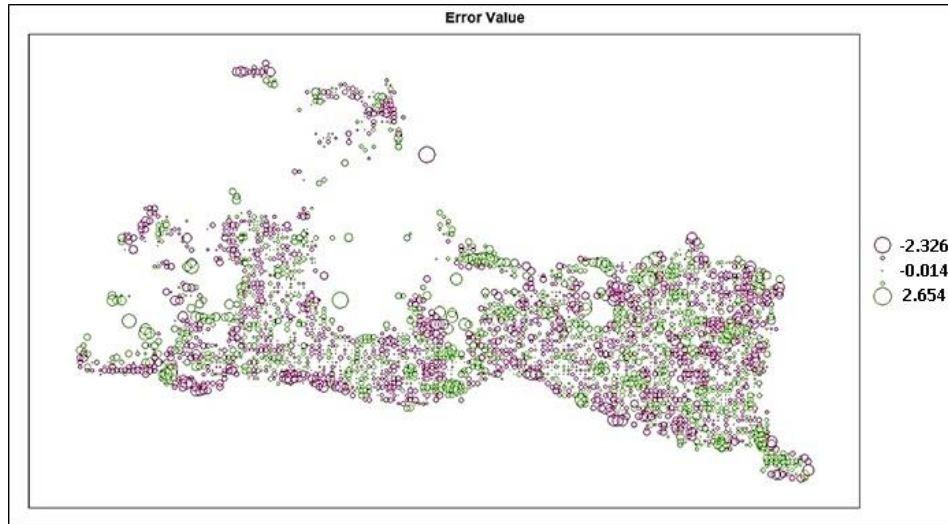


Figure 4. Distribution of error value with 70% of qualified pixels used for validation

Table 5. Spatial correlation coefficient

Aggregate of band 13	Skin temperature	Correlation coefficient
December-February	February	0.703
March-May	May	0.801

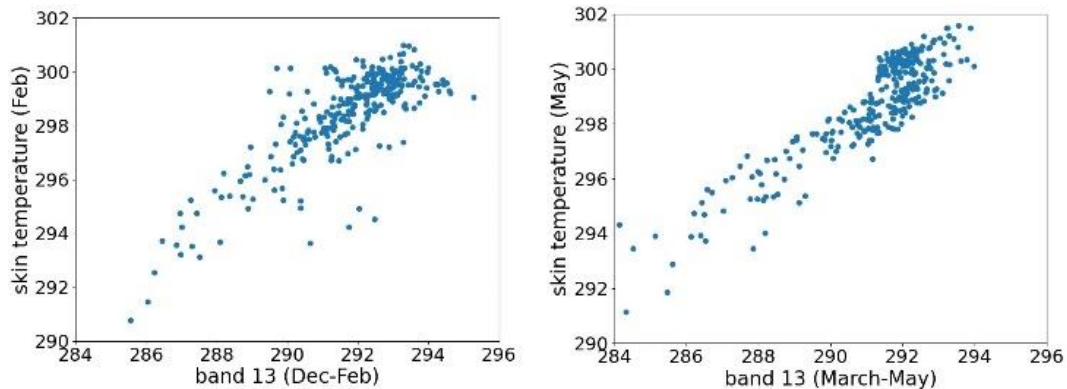


Figure 5. Scatter diagram of interpolated data and skin temperature from ERA5

Although the result shows good behavior, evaluation of data distribution in the time domain is still needed. Different weights for different periods of time due to data availability might be applied like in [26]. The spatial distribution pattern of data should also be clearly identified to improve the criteria in the spatial domain.

4. CONCLUSION

Full spatial resolution of aggregate data over the east part of Java could be obtained in shorter regular periods than over the west part of Java. Time series aggregate data could be potentially created by dividing the data into three-month periods using hourly Himawari-8 images, while over the western part of Java the length of period could be up to six months. The result of this study increases confidence in using optical remote sensing images from the Himawari-8 satellite to create time series data over a region. Comparison to the use of 10-minute HCAI data in future research might provide more robust results. For a more precise result, better criteria on data distribution patterns in both the time domain and the spatial domain should also be considered.

ACKNOWLEDGEMENTS

The authors would like to thank the Indonesian National Research and Innovation Agency (BRIN) for providing financial support for this research under the Saintek 2018 Scholarship Program. We also express our gratitude to the Indonesian Meteorological, Climatological, and Geophysical Agency (BMKG) and also to the Japan Aerospace Exploration Agency (JAXA) for providing Himawari-8 satellite data.

REFERENCES

- [1] C. K. Yang, F. P. Shan, and T. L. Tien, "Climate change detection in Penang island using deterministic interpolation methods," *Indones. J. Electr. Eng. Comput. Sci.*, vol. 19, no. 1, pp. 412–419, 2020, doi: 10.11591/ijeecs.v19.i1.pp412-419.
- [2] K. F. Fung *et al.*, "Evaluation of spatial interpolation methods and spatiotemporal modeling of rainfall distribution in Peninsular Malaysia," *Ain Shams Eng. J.*, vol. 13, no. 2, p. 101571, 2022, doi: 10.1016/j.asej.2021.09.001.
- [3] S. M. S. Shah, M. El-Morshedy, and W. Mansoor, "Spatial-temporal interpolation of reference evapotranspiration for Pakistan," *Math. Probl. Eng.*, vol. 2022, 2022, doi: 10.1155/2022/5488725.
- [4] R. R. E. Vernimmen, A. Hooijer, Mamenun, E. Aldrian, and A. I. J. M. Van Dijk, "Evaluation and bias correction of satellite rainfall data for drought monitoring in Indonesia," *Hydrol. Earth Syst. Sci.*, vol. 16, no. 1, pp. 133–146, 2012, doi: 10.5194/hess-16-133-2012.
- [5] A. K. Whitcraft, E. F. Vermote, I. Becker-Reshef, and C. O. Justice, "Cloud cover throughout the agricultural growing season: Impacts on passive optical earth observations," *Remote Sens. Environ.*, vol. 156, pp. 438–447, 2015, doi: 10.1016/j.rse.2014.10.009.
- [6] J. P. Gastellu-Etchegorry, "Cloud cover distribution in Indonesia," *Int. J. Remote Sens.*, vol. 9, no. 7, pp. 1267–1276, 1988, doi: 10.1080/01431168808954934.
- [7] R. D. Dimiyati, P. Danoedoro, Hartono, and Kustiyo, "A minimum cloud cover mosaic image model of the operational land imager landsat-8 multitemporal data using tile based," *Int. J. Electr. Comput. Eng.*, vol. 8, no. 1, pp. 360–371, 2018, doi: 10.11591/ijece.v8i1.pp360-371.
- [8] K. Islam, M. F. Rahman, and M. Jashimuddin, "Modeling land use change using cellular automata and artificial neural network: The case of chunati wildlife sanctuary, Bangladesh," *Ecol. Indic.*, vol. 88, no. May 2017, pp. 439–453, 2018, doi: 10.1016/j.ecolind.2018.01.047.
- [9] C. Liping, S. Yujun, and S. Saeed, "Monitoring and predicting land use and land cover changes using remote sensing and GIS techniques—A case study of a hilly area, Jiangle, China," *PLoS One*, vol. 13, no. 7, pp. 1–23, 2018, doi: 10.1371/journal.pone.0200493.
- [10] C. Rankine, G. A. Sánchez-Azofeifa, J. A. Guzmán, M. M. Espirito-Santo, and I. Sharp, "Comparing MODIS and near-surface vegetation indexes for monitoring tropical dry forest phenology along a successional gradient using optical phenology towers," *Environ. Res. Lett.*, vol. 12, no. 10, 2017, doi: 10.1088/1748-9326/aa838c.
- [11] H. Sun, W. Liu, Y. Wang, and S. Yuan, "Evaluation of typical spectral vegetation indices for drought monitoring in cropland of the North China plain," *IEEE J. Sel. Top. Appl. Earth Obs. Remote Sens.*, vol. 10, no. 12, pp. 5404–5411, 2017, doi: 10.1109/JSTARS.2017.2734800.
- [12] M. Neteler, "Estimating daily land surface temperatures in mountainous environments by reconstructed MODIS LST data," *Remote Sens.*, vol. 2, no. 1, pp. 333–351, 2010, doi: 10.3390/rs1020333.
- [13] J. Yang and M. Hu, "Filling the missing data gaps of daily MODIS AOD using spatiotemporal interpolation," *Sci. Total Environ.*, vol. 633, pp. 677–683, 2018, doi: 10.1016/j.scitotenv.2018.03.202.
- [14] H. He, J. Yan, L. Wang, D. Liang, J. Peng, and C. Li, "Bayesian temporal tensor factorization-based interpolation for time-series remote sensing data with large-area missing observations," *IEEE Trans. Geosci. Remote Sens.*, vol. 60, pp. 1–13, 2022, doi: 10.1109/TGRS.2022.3140436.
- [15] J. Zhou, L. Jia, and M. Menenti, "Reconstruction of global MODIS NDVI time series: Performance of harmonic analysis of time series (HANTS)," *Remote Sens. Environ.*, vol. 163, pp. 217–228, 2015, doi: 10.1016/j.rse.2015.03.018.
- [16] Y. Luo, Y. Zhang, X. Cai, and X. Yuan, "E2GAN: End-to-end generative adversarial network for multivariate time series imputation," *IJCAI Int. Jt. Conf. Artif. Intell.*, vol. 2019-Augus, 2019, pp. 3094–3100, doi: 10.24963/ijcai.2019/429.
- [17] H. Suzue, T. Imai, and K. Mouri, "High-resolution cloud analysis information derived from Himawari-8 data," *Meteorol. Satell. Cent. Tech. Note*, vol. 43, no. 61, pp. 43–51, 2016.
- [18] O. Gustin, R. U. Manik, F. D. Rassarandi, A. Roziqin, N. H. Isya, and T. C. Krisna, "Land surface temperature identification based on data of landsat 8 on batam Island," *Proc. ICAE 2020 - 3rd Int. Conf. Appl. Eng.*, no. 2, pp. 8–13, 2020, doi: 10.1109/ICAE50557.2020.9350552.
- [19] Y. D. Vybornoova, "Application of spatial interpolation methods for restoration of partially defined images," *CEUR Workshop Proc.*, vol. 2210, pp. 89–95, 2018, doi: 10.18287/1613-0073-2018-2210-89-95.
- [20] G. Simpson and Y. H. Wu, "Accuracy and effort of interpolation and sampling: Can GIS help lower field costs?," *ISPRS Int. J. Geo-Information*, vol. 3, no. 4, pp. 1317–1333, 2014, doi: 10.3390/ijgi3041317.
- [21] A. A. Ibrahim, I. M. Farhan, and M. E. Safi, "A nonlinearities inverse distance weighting spatial interpolation approach applied to the surface electromyography signal," *Int. J. Electr. Comput. Eng.*, vol. 12, no. 2, pp. 1530–1539, 2022, doi: 10.11591/ijece.v12i2.pp1530-1539.
- [22] R. Yang and B. Xing, "A comparison of the performance of different interpolation methods in replicating rainfall magnitudes under different climatic conditions in chongqing province (China)," *Atmosphere (Basel)*, vol. 12, no. 10, 2021, doi: 10.3390/atmos12101318.
- [23] Yanto, A. Apriyono, P. B. Santoso, and Sumiyanto, "Landslide susceptible areas identification using IDW and Ordinary Kriging interpolation techniques from hard soil depth at middle western Central Java, Indonesia," *Nat. Hazards*, vol. 110, no. 2, pp. 1405–1416, 2022, doi: 10.1007/s11069-021-04982-5.
- [24] Y. Yamamoto, H. Ishikawa, Y. Oku, and Z. Hu, "An algorithm for land surface temperature retrieval using three thermal infrared bands of Himawari-8," *J. Meteorol. Soc. Japan*, vol. 96B, no. November 2017, pp. 59–76, 2018, doi: 10.2151/jmsj.2018-005.
- [25] S. Zareie, K. Rangzan, H. Khosravi, and V. M. Sherbakov, "Comparison of split window algorithms to derive land surface temperature from satellite TIRS data," *Arab. J. Geosci.*, vol. 11, no. 14, 2018, doi: 10.1007/s12517-018-3732-y.
- [26] Y. Zhang, W. Jiang, and X. Deng, "Fault diagnosis method based on time domain weighted data aggregation and information fusion," *Int. J. Distrib. Sens. Networks*, vol. 15, no. 9, 2019, doi: 10.1177/1550147719875629.

BIOGRAPHIES OF AUTHORS

Ahmad Luthfi Hadiyanto    is a doctoral student at the Department of Geodesy and Geomatics Engineering, Bandung Institute of Technology, Indonesia. He works at the Indonesian National Research and Innovation Agency. He supervised satellite data processing activities at a remote sensing ground station. He also held administrative positions before continuing his doctoral studies. His research interests include remote sensing, artificial intelligence, and data science. He received a bachelor's degree in electrical engineering from Bandung Institute of Technology in 2002 and an M.Sc. degree in space technology application from Beihang University, China, in 2010. He can be contacted by email at: luthfi.hadiyanto@students.itb.ac.id.



Ketut Wikantika    is a Professor in Environmental Remote Sensing in the Department of Geodesy and Geomatics Engineering, Bandung Institute of Technology, Indonesia. His research focuses on geospatial approaches, including remote sensing applications for demography, agriculture, forestry, land use and landcover change, biogeography, biodiversity, and disaster mitigation. He received a bachelor's degree in geodesy and geomatics engineering from Bandung Institute of Technology; a Master of Engineering degree in image informatics from Chiba University, Japan; and a Ph.D. degree in remote sensing from Chiba University, Japan. In doing his research, he built collaborations with national and international institutions, i.e., Chiba University, Tottori University, Nagoya University, Kochi University, JIRCAS Japan, Oklahoma University, AIT, Salzburg University, UTM Malaysia, and Pennsylvania State University. He can be contacted by email at: ketut@gd.itb.ac.id.



Ary Setijadi Prihatmanto    is the Director of the Research Center on Information and Communication Technology at the Research and Innovation Building, Bandung Institute of Technology, Indonesia. He received his bachelor's and master's degrees in electrical engineering from Bandung Institute of Technology. In 2006, he received his Ph.D. degree in Applied Informatics from Johannes Kepler University of Linz, Austria. His research interests include human-content interaction, virtual reality and mixed reality, brain-computer interaction, modelling and simulation, and artificial intelligence. He can be contacted by email at: asetijadi@lisk.ee.itb.ac.id.



Nurjanna Joko Trilaksono    is a lecturer at the Faculty of Earth Science and Technology, Bandung Institute of Technology, Indonesia. His research interests include mesoscale meteorology and modelling in meteorology. He received his bachelor's degree in meteorology and his master's degree in earth science from Bandung Institute of Technology. In 2012, he received his Ph.D. degree from the Department of Geophysics, Kyoto University, Japan. He can be contacted by email at: jpatiani@meteo.itb.ac.id.



Dedi Irawadi    is a senior engineer at the Indonesian National Research and Innovation Agency. He received his B.Sc. degree in electrical engineering from Texas A&M University, USA. He is an expert in remote sensing technology, including ground stations, satellite telecommunications, and data centers. He was the Ground Station Manager of the Indonesian Nasional Institute of Aeronautics and Space in 2007-2013. He was also the Director of Remote Sensing Technology and Data Center from 2014 to 2021. He can be contacted by email at: dedi.irawadi@brin.go.id.